GEORGIA TECH
FUSION RESEARCH CENTER
ANNUAL REPORT
2011

Prepared by
Weston M. Stacey
September, 2011

Summary The Georgia Tech work i) on interpretation of the DIII-D experiment and ii) on the development of the fission-fusion hybrid burner reactor (SABR) concept is described.

I.   ***COLLABORATION ON INTERPRETATION OF DIII-D EXPERIMENTS***
         (Supported by DoE-OFES Grant DE-FG02-99ER54538)

A.   EDGE PEDESTAL STRUCTURE DETERMINED BY THE PARTICLE, MOMENTUM AND ENERGY BALANCES AND THE HEAT CONDUCTION RELATION

W. M. Stacey (Georgia Tech), R. J. Groebner and T. E. Evans (General Atomics)

The possibility that the density, temperature and pressure profiles in the edge pedestal are determined by the first four fluid moments of the Boltzman transport equation, with appropriately determined constitutive relations, has been investigated on DIII-D. The following formalism has been developed and applied to a variety of DIII-D discharges

The first moment is the continuity, or particle balance equation for the main ion species "j"

$$\frac{\partial (n_j V_{rj})}{\partial r} = -\frac{\partial n_j}{\partial t} + n_e n_o \langle \sigma v \rangle_{ion} + S_{nb} \tag{1}$$

whch determines the radial particle flux $\Gamma_j = n_j V_{rj}$, where V_{rj} is the radial ion particle flux, the second term on the right is the ionization of recycling neutrals and the last term is the neutral beam source.

The toroidal and radial components of the second moment, or momentum balance, equation can be combined to obtain an equation that determines the pressure profile

$$-\frac{1}{p_j}\frac{\partial p_j}{\partial r} = \frac{V_{rj} - V_{rj}^{pinch}}{D_j} \tag{2}$$

where the "diffusion coefficient"

$$\widehat{D}_j \equiv \frac{m_j T_j \nu_{jk}}{\left(e_j B_\theta\right)^2}\left(1 + \frac{\nu_{dj}}{\nu_{jk}} - \frac{e_j}{e_k}\right) \tag{3}$$

and the "pinch velocity"

$$V_{rj}^{pinch} \equiv \frac{\left[-M_{\phi j} - n_j e_j E_\phi^A + n_j m_j \left(\nu_{jk} + \nu_{dj}\right)\left(f_p^{-1}V_{\theta j} + E_r/B_\theta\right) - n_j m_j \nu_{jk} V_{\phi k}\right]}{n_j e_j B_\theta} \tag{4}$$

is a collection of normalized forces associated with the electric field, *VxB* forces and beam momentum input. The quantity ν_{dj} is a toroidal angular momentum transfer frequency which represents the combined effect of viscosity, inertia, atomic physics, and other "anomalous" processes, which can be inferred from experiment. (These equations are written for the main ion species "j" in a two-species plasma with impurity species "k".)

The third moment, or energy balance equations for the main ion and electron species

$$\frac{\partial Q_j}{\partial r} \equiv \frac{\partial}{\partial r}\left(q_j - \frac{3}{2}\Gamma_j T_j\right) = -\frac{\partial}{\partial t}\left(\frac{3}{2}n_j T_j\right) + q_{nbj} - q_{je} - n_e n_o^c \langle\sigma\upsilon\rangle_{cx}\frac{3}{2}\left(T_j - T_o^c\right) \quad (5)$$

and

$$\frac{\partial Q_e}{\partial r} \equiv \frac{\partial}{\partial r}\left(q_e - \frac{3}{2}\Gamma_e T_e\right) = -\frac{\partial}{\partial t}\left(\frac{3}{2}n_e T_e\right) + q_{nbe} + q_{je} - n_e n_k L_k(T_e) \quad (6)$$

determine the main ion and electron total energy fluxes, $Q_{j,e}$, from which the conductive heat fluxes, $q_{j,e}$, can be determined. The q_{nb} terms represent neutral beam (or other) heating, q_{je} is the ion-to-electron collisional energy transfer, and the last terms in Eqs. (5) and (6) represent charge-exchange cooling of the ions and radiation cooling of the electrons, respectively.

Finally, the heat conduction relations

$$q_{j,e} = -n_{j,e}\chi_{j,e}\frac{\partial T_{j,e}}{\partial r} \quad (7)$$

can be used as a surrogate for the fourth moment, or energy flux, equation to determine the temperature profiles.

If the viscous component of the angular momentum transfer frequencies $\nu_{dj,k}$ and the thermal diffusivities $\chi_{j,e}$ were known, from. kinetic theory or fluctuation theory or experiment, it should be possible to solve Eq. (2) for the pressure distribution and Eq. (7) for the temperature distribution, then construct the ion distribution from $n = p/T$. We have investigated this conjecture for a variety of DIII-D shots by using measured rotation velocities, electric fields and other quantities to evaluate the RHS of Eq(2). Figure 1 shows the radial velocity calculated from Eq. (1) and the pinch velocity evaluated from experimental data for an ELMing H-mode discharge that has been much analyzed. When these "velocities" were used to integrate Eq. (2) and the resulting pressure was divided by the experimental ion temperature and then corrected for impurities, the electron density shown in Figure 2 was obtained. The measured electron density profile is shown for comparison.

The effect of the *VxB, Erad* and other "physics" forces on the determination of the pressure profile from Eq. (2) enters through the term V_{rj}^{pinch}, which was evaluated mostly from experimental data The effect of recycling neutrals on the determination of the pressure profile from Eq. (2) enters through the term V_{rj}, which is evaluated by solving Eq. (1). Thus, comparing these two terms in Fig. 1 provides an appreciation of the relative importance of recycling neutrals and *VxB, Erad* and other forces on the determination of the pressure profile. Similar results have been found in other discharges.

The effect of the *VxB, Erad* and other "physics" forces on the determination of the pressure profile from Eq. (2) enters through the term V_{rj}^{pinch}, which was evaluated mostly from experimental data The effect of recycling neutrals on the determination of the pressure profile from Eq. (2) enters through the term V_{rj}, which is evaluated by solving Eq. (1). Thus,

comparing these two terms in Fig. 1 provides an appreciation of the relative importance of recycling neutrals and *VxB, Erad* and other forces on the determination of the pressure profile.

This same type of analysis has been applied to understand (in terms of differences in the edge radial electric field rotation velocities and the resulting differences in particle pinch) the differences in density profiles between "matched" H-mode and RMP discharges[1], the evolution of density and temperature profiles between ELMS[2], and the difference in density and temperature profiles across an L-H transition[3].
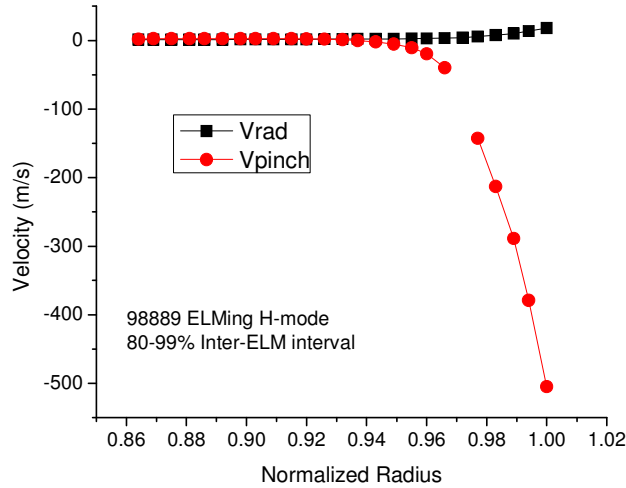

Figure 1   Comparison of the effects of recycling neutrals (V_{rad}) and *VxB* and *Erad* (*Vpinch*) in determining the pressure gradient in the edge pedestal.
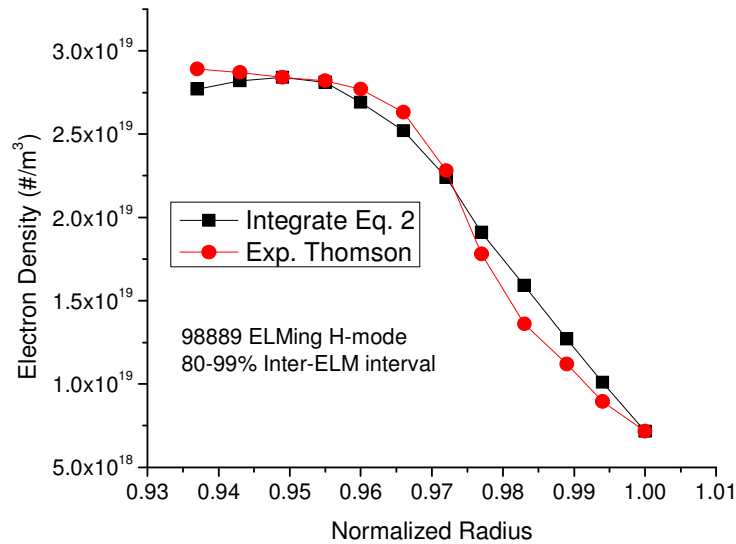

Figure 2 Comparison of measured and calculated ion density profile in edge pedestal.

1. W. M. Stacey and T. E. Evans, "The role of radial particle pinches in ELM suppression by resonant magnetic perturbations", *Nucl. Fusion* 51, (2011).

2. W. M. Stacey and R. J. Groebner, "Evolution of the H-mode edge pedestal between ELMs", *Nucl. Fusion* 51, 063024 (2011).
3. W. M. Stacey and R. J. Groebner, "Force balance and ion particle transport differences in high and low confinement tokamak edge pedestals", *Phys. Plasmas* 17, 112512 (2010).

B. ION ORBIT LOSS AND X-LOSS

W. M. Stacey, Georgia Tech.

Models have been developed for the calculation of i) standard ion orbit loss across the separatrix and of ii) X-loss of ions in the narrow, null-B_θ region extending into the plasma from the X-point in a divertor plasma, which are trapped poloidallly while they gradB drift radially outward through the X-point region. Calculations of a DIII-D discharge indicate a significant non-diffusive transport ion and ion energy loss in the edge pedestal due to these loss mechanisms. Taking this particle and energy loss into account when determining the conductive ion energy flux results in a significant reduction in the experimental thermal diffusivity interpreted from the measured temperature profile.
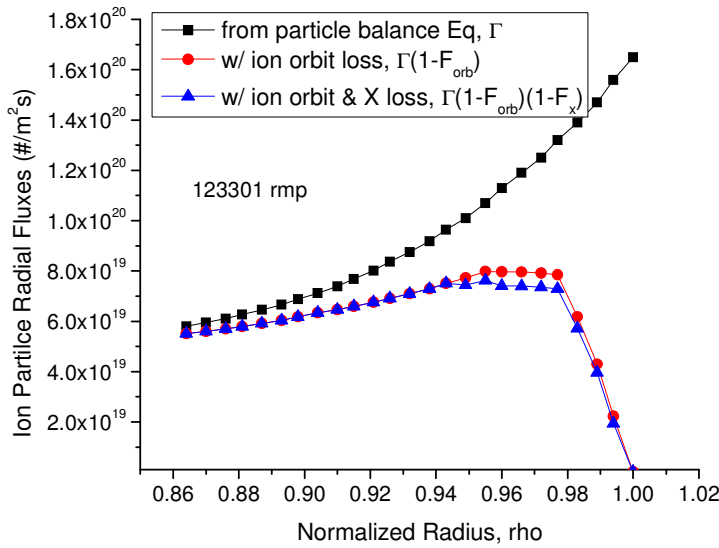

Figure 1   Convective/diffusive ion particle fluxes with and without ion orbit loss and X-loss (F_{orb} and F_x are ion orbit loss and X-loss particle flux reduction factors)
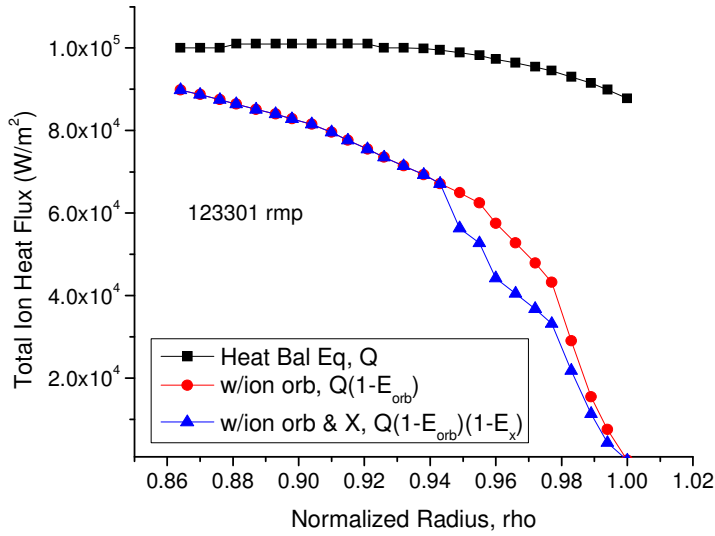
Figure 2   Total ion heat flux calculated from ion heat balance equation and corrected for ion orbit and X-loss. (E_{orb} and E_x are ion orbit loss and X-loss ion energy flux reduction factors)

The effect of ion orbit loss and X-loss on heat and particle fluxes propagates into the interpretation of the experimental ion heat diffusivity from measured density and ion temperature data, as shown in Fig. 3.
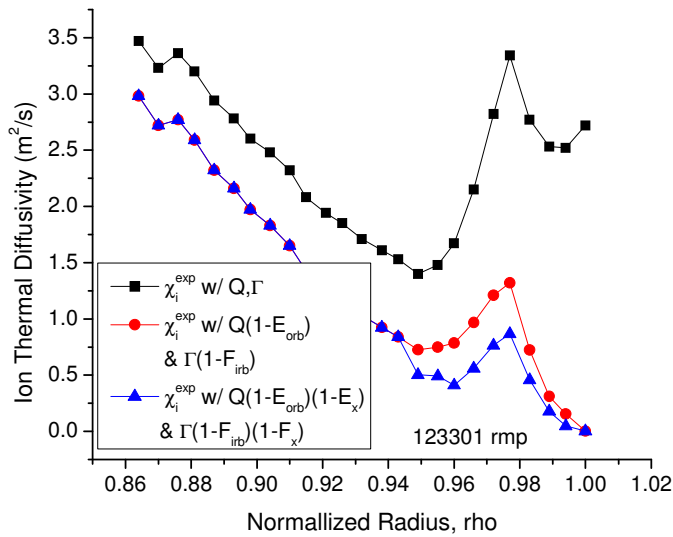

Figure 3   Ion thermal diffusivities interpreted from the measured ion temperature profile using Eq. (23) and the heat fluxes of Fig. 5 with   and without ion orbit loss.

1. W. M. Stacey, "The effect of ion orbit loss on the interpretation of ion energy and particle transport in the DIII-D edge plasma", *Phys. Plasmas,* (to be published 2011).

C.   X-TRANSPORT IN DIVERTED TOKAMAKS
W. M. Stacey, Georgia Tech

A methodology for treating within fluid codes the X-transport produced by the outward grad-B and curvature drifts of ions trapped poloidally in the null- X-region about the X-point in diverted tokamak plasmas was presented. The X-transport is sensitive to the radial electric field and ion temperature profiles at the location of the X-region in the edge pedestal just above the X-point. This X-transport formalism was applied to two DIII-D discharges. It was found that X-transport is a significant contributor to the ion radial particle and heat fluxes in these discharges. From this it can be concluded that X-transport should be taken into account in both predictive and interpretive analyses of the edge pedestal in diverted tokamaks.

1.   W. M. Stacey, "X-transport of ions in diverted tokamaks, with application to DIII-D", *Phys. Plasmas*, (submitted 2011).

D.   NUMERICAL INVESTIGATION OF THE PINCH-DIFFUSION EQUATION
J-P. Floyd and W.M. Stacey, Georgia Tech

Radial and toroidal momentum balance requires the ion particle flux in the edge pedestal to satisfy a pinch-diffusion relation, $\Gamma = -D\nabla n + nV_r^{pinch}$, rather than the pure diffusion relation used to derive standard diffusion theory. Re-derivation of diffusion theory by using the pinch diffusion relation in the particle continuity equation yields a generalized diffusion equation[1] which, in principle, can be solved by modifying the standard diffusion theory methods and codes. We have investigated this possibility by using standard finite difference and Gauss reduction solution procedures for 1D diffusion theory to solve this equation. Analysis of the equation yields an expression for the numerical error of various finite-difference algorithms proportion to the square of the ratio Δ of the mesh spacing to the characteristic scale length, $L \equiv \left| D_j / V_{rj}^{pinch} \right|$.

$$error \cong \frac{1}{2}\left(\frac{\Delta}{L}\right)^3 \begin{cases} 1 - \frac{1}{3}\frac{\Delta}{L} + ... & backward\ difference \\ 1 & central\ difference \\ 1 + \frac{1}{3}\frac{\Delta}{L} + ... & forward\ difference \end{cases}$$

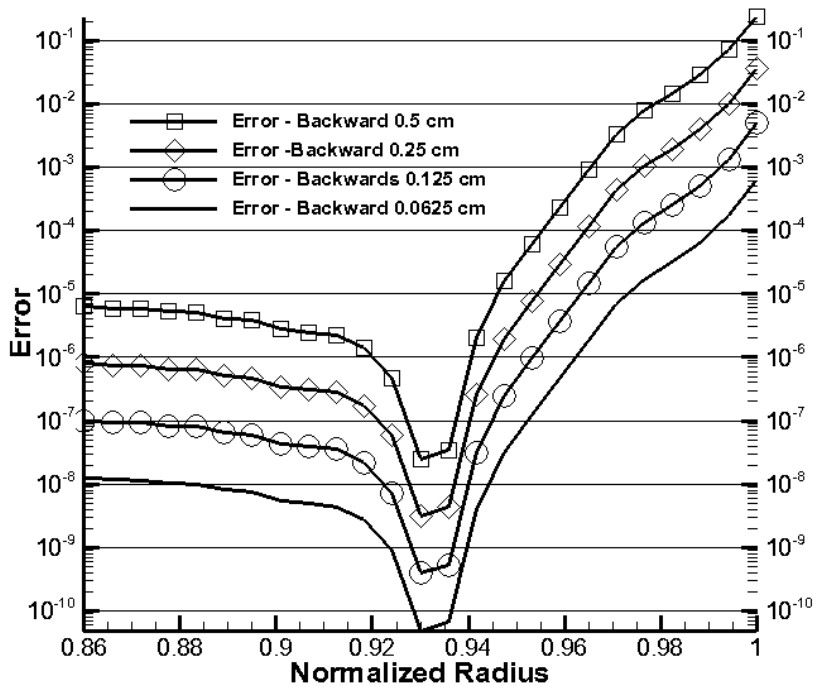This quantity is plotted in Fig. 1 for DIII-D shot 98889.

Figure 1   Error in pinch-diffusion numerical approximation.

The implication of this result is that smaller mesh spacing will be necessary in the edge pedestal, where the inward pinch velocity is large, than is necessary for similar accuracy further inward, where the pinch velocity diminishes. This result was confirmed by numerical solution of the equation for a DIII-D shot. Details are described in Ref. 2.

1. W. M. Stacey, "Ion Particle Transport in the Tokamak Edge Plasma". *Contrib. Plasma Phys.* **48,** 94 (2008).

2. J-P. Floyd and W. M. Stacey, "Numerical Investigation of the Generalized Pinch-Diffusion Equations in the Edge Pedestal", *Fusion Sci. & Technol.* (to be published 2011).

E.   **NEOCLASSICAL THEORY FOR TOROIDAL AND POLOIDAL ROTATION**

C. Bae and W. M. Stacey (Georgia Tech) and W. M. SOLOMON (Princeton Plasma Physics Laboratory)

Rotation of tokamak plasmas is of intrinsic interest and also important for stabilization of MHD modes. Neoclassical rotation theory and gyroviscosity both depend on the poloidal dependence of the magnetic flux surface geometry. The circular ($R = R_0(1 + \varepsilon \cos \theta), B = B_0 / (1 + \varepsilon \cos \theta)$) flux surface formulation (Phys. Plasmas 13, 062508, 2006) was found to overpredict toroidal rotation velocities in DIII-D by a factor of about 2. We have developed a new representation of neoclassical plasma rotation theory in the more accurate

7

"Miller equilibrium" flux surface geometry (Phys. Plasmas 5, 973, 1998). The Miller model takes into account Shafranov shift, elongation, and triangularity. Development of the neoclassical plasma rotation theory for both the circular or Miller equilibrium models is now complete, and the resulting solution procedure for the coupled non-linear.equations is in progress.

When completed, the new calculation will be compared against a pair of co-rotating and counter-rotating DIII-D discharges. Assembling of the experimental data for this comparison is in progress.

II.   *ANALYSES OF FUSION-FISSION HYBRID REACTORS*

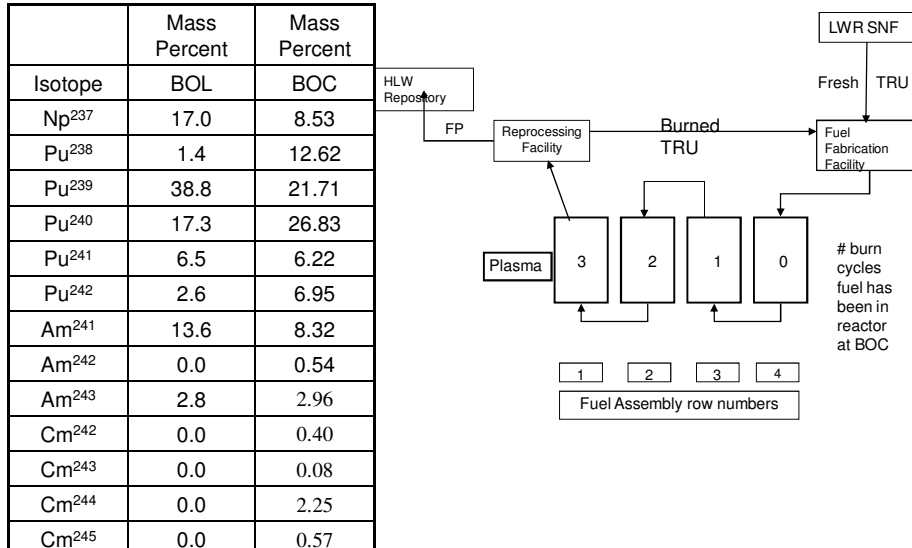## A.   FUEL CYCLE ANALYSES OF THE SUBCRITICAL ADVANCED BURNER REACTOR (SABR)
C. M. Sommer, W. M. Stacey and B. Petrovic, Georgia Tech

SABR TRU Burner Fuel Cycle in Support of LWRs

The reference SABR fuel cycle[1] is indicated in Fig. 1. The fuel assemblies are first loaded in the outermost ring 4, burned for one burn cycle, then moved inward to ring 3, burned for one burn cycle, etc. until they have been burned for four burn cycles, at which point they are removed from the innermost ring 1 and sent to the reprocessing facility for separation of the remaining transuranics from the fission products. The separated transuranics (plus 1% of the fission products) are then sent back to the fuel fabrication facility where they are mixed with "fresh" transuranics (TRU) taken directly from LWR spent fuel and recycled back through the burner reactor again. At the beginning of operation (BOL) the fuel in all four rings has the composition of the spent nuclear fuel removed from LWRs, but after a few such cycles the composition of the fuel entering ring 4 at beginning of cycle (BOC) and the composition of the fuel removed from ring 1 at end of cycle (EOC) and sent for reprocessing both reach an equilibrium composition. The fuel residence time of 2800 full power days (fpd) in SABR is set by the 200 dpa clad radiation damage limit, and each burn cycle is one-fourth of this residence time, or 700 fpd. With this type of repeated reprocessing of the burner reactor discharge fuel, all of the transuranics are eventually destroyed, except for the 1% that go to the HLWR with the fission products on each reprocessing step because of separation inefficiency. The decay heat in the HLWR at 100,000 years is reduced to 3.5% of the value that would be present if the spent nuclear fuel from LWRs was placed directly in the HLWR, indicating about a 30-fold reduction in the required HLWR capacity relative to direct burial of the discharged LWR spent fuel.

SABR TRU BURNER Fuel Cycle

ANL Fuel Composition

Isotope	Mass Percent BOL	Mass Percent BOC
Np^{237}	17.0	8.53
Pu^{238}	1.4	12.62
Pu^{239}	38.8	21.71
Pu^{240}	17.3	26.83
Pu^{241}	6.5	6.22
Pu^{242}	2.6	6.95
Am^{241}	13.6	8.32
Am^{242}	0.0	0.54
Am^{243}	2.8	2.96
Cm^{242}	0.0	0.40
Cm^{243}	0.0	0.08
Cm^{244}	0.0	2.25
Cm^{245}	0.0	0.57

Figure 1. SABR 4-Batch Fuel Cycle with Out-to-In Fuel Shuffling

With the initial BOL composition containing 30.3 MT of TRU, k_{eff} = 0.945 and P_{fus} = 172 MWth is needed to provide enough fusion neutrons to produce 3000MWth power in the fission reactor core (from fission, exoergic reactions and the slowing down of fusion neutrons). Once the equilibrium fuel cycle is reached, at BOC k_{eff} =0.878, P_{fus}= 312 MW, TRU=28.8MT, and at EOC k_{eff}=0.831, P_{fus}=409 MW, TRU= 26.8MT. In the equilibrium fuel cycle, 1.06 MT of TRU is fissioned every full-power year (fpy).

Since a 1000 MWe LWR also produces about 3000MWth power and 0.25 MT/y TRU, the support ratio for SABR is 3.2 at 75% availability (4.2 at 100% availability). Thus, one could envision a reactor fleet of LWRs producing 75% of the power and SABRs producing 25% of the power by burning all the TRU produced in the LWRs.

SABR Minor Actinide Burner Fuel Cycle in Support of a Transition to a Fast Reactor Fleet

If some of the plutonium is separated from the TRU discharged from LWRs to use to start up fast reactors at a later date, this leaves a minor actinide (MA) rich composition of transuranics to be fissioned in fast burner reactors. We have investigated a similar 4-batch burner reactor fuel cycle based on the BOL fuel composition which is used in European studies of this situation. The MA-rich TRU-oxide fuel (with some Pu removed) is less reactive than the TRU fuel shown above, and it was necessary to slightly redesign the SABR fuel assemblies to accommodate this fuel while remaining within the same general range of k_{eff} and P_{fus} discussed above.

The fuel cycle[7] was similar to that depicted in Fig. 1, except for Pu being removed from the LWR SNF. At beginning of operation (BOL) k_{eff}=0.889, P_{fus}=470 MW, TRU = 50.0MT, while at the beginning of equilibrium cycle (BOC) k_{eff}=0.949, P_{fus}=195 MW, TRU = 48.5MT and at the end of equilibrium cycle k_{eff}=0.932, P_{fus}=289 MW, TRU = 46.5MT. In the equilibrium fuel cycle 1.08 MT/fpy of TRU (0.85 MT/fpy of MA) is fissioned. Since a 1000MWe LWR produces

0.025 MT/y of MA, the support ratio for SABR at 75% availability is 25.5 in this fuel cycle. Thus, a nuclear power fleet of 96% LWRs supported by 4% SABRs to burn the minor actinides would be envisioned in this "transition to fast reactors" scenario. The decay heat in the HLWR at 100,000 years is reduced to 11% of the value that would be present if the spent nuclear fuel from LWRs was placed directly in the HLWR after some plutonium was removed to be saved for fast reactor startup, indicating a 10-fold reduction in the required HLWR capacity.

1. C.M. Sommer, W. M. Stacey, B. Petrovic, Nucl. Technol. 172, 48 (2010); Nucl. Technol. (to be published 2011).

B. SCENARIO STUDIES OF MINOR ACTINIDE DESTRUCTION
C. M. Sommer, W. M. Stacey and B. Petrovic (Georgia Tech) and V. Romanelli, M. Salvatores, W. Maschek, F. Gabrielli, B. Vezzoni, A. Schwenk-Ferrero and A. Rineiski (Karlsruhe Institute of Technology)

The "double-strata" strategy being developed for the management of spent nuclear fuel (SNF) in Europe envisions removing some of the plutonium from the SNF and then disposing of the remaining minor actinide (MA) rich transuranics either in a Low-Conversion-Ratio critcal Fast Reactor (LCRFR), a subcritical fast reactor driven by an accelerator neutron source (EFIT) or in a subcritical fast react driven by a fusion neutron source (SABR). Initial investigations based on the SNF in Europe indicate that all three types of transmutation reactors would capable of stabilizing the minor actinide content in the European spent nuclear fuel by 2150[1,2].

Applying the same type of transmutation rates to the minor actinides being produced by the present US LWR fleet indicates 10 (1000MWth) LCRFRs, or 19 (384MWth) EFITs, or 4 (3000MWth) SABRs would be required to destroy the annual minor actinide production in the present US fleet of LWRs.

1. V. Romanello, C. Sommer, M. Salvatores, W. Stacey, et al., "Advanced Fuel Cycle Scenario in the European Context by Using Different Burner Reactor Concepts", Proc. 11th OECD/NEA Information Exchange Meeing of Actinide Partitioning and Transmutation (2011).
2. V. Romaneloi, M. Salvatores, W. Stacey, et. al., "Comparison of Waste Transmutation Potential of Different Innovative Dedicated Systems and Impact on Fuel Cycle", Proc. ICENES-2011 (2011).

C. DYNAMIC SAFETY STUDIES OF SABR
A.Bopp and W. M. Stacey, Georgia Tech

The previous SABR dynamic safety analyses (Nucl. Technol. 171, 123, 2010) are being extended to include the fuel bowing reactivity coefficient which is important for passive safety. A model for this reactivity coefficient and for the fuel motion with temperature is being developed, based on consultation with Argonne National Laboratory staff. The immediate objective of this work is to determine if SABR retains the passive safety against LOCA and LOHSA of the IFR, or if it can be modified to achieve this passive safety.

The ultimate objective of the dynamic safety analysis effort is to establish a metric for determining the "safety equivalence" of critical reactors with different TRU fuel fractions vs SABRs with different subcriticalities. This is necessary in order to establish the basis for comparison of "safety comparable" critical and sub-critical burner reactors.

D.   FUEL CYCLE STUDIES OF SUBCRITICAL ADVANCED BREEDER REACTOR

C. Stewart, W. M. Stacey and B. Petrovic, Georgia Tech

Investigation has begun into the capacity of SABR as a breeder reactor using the ERANOS fast reactor physics code. The SABR breeder concept is a sodium-cooled, U-Pu-Zr fueled, subcritical fast reactor with a tokamak fusion neutron source. The IFR fuel pins have been adopted so as to facilitate a comparison with a developed critical system. The primary expected advantages come from a reactivity safety margin to prompt critical an order of magnitude greater than that in critical fast systems, from lifting the requirement for flat reactivity over fuel residence time, and from the introduction of 14.1 MeV neutrons from the fusion source into the spectrum.

The driver fuel is ~22 wt% ANL Pu vector (which is ~68% fissile isotopes) mixed with 0.25%wt tails Uranium, and the blankets (radial and upper and lower axial) are entirely DU; each is mixed at 90 wt% heavy metal to 10 wt% Zr. The BOL k_{eff} is 0.948, which drops to 0.933 by EOC; there is still slight headroom in the BOL k_{eff} to increase driver enrichment for the purposes of increasing cycle length or altering driver/blanket loading.

The current issues being studied concern a power peaking at the plasma-side edge of the fission region and achieving a tritium breeding ratio adequate for tritium self-sufficiency. The power peak grows as Pu is bred into the inboard blanket, but even by EOC barely surpasses the power in the driver fuel. More Lithium blankets are being added to the areas surrounding the plasma and the underside of the fission core in order to increase tritium breeding.

The plasma source is kept near its 500MW maximum output in order to maximize the contribution of the high-energy fusion neutrons to the spectrum at the inboard edge of the fission region. Fuel residence time is currently constrained by the ability of the plasma to drive the subcritical reaction – radiation damage limits of the cladding do not appear to be a limiting issue at this point. The composition of the inner ring of assemblies disproportionately affects the multiplication of the source neutrons, and thus the drivability of the fission core, and will consequently heavily influence any decisions on refueling schemes.

E.   Presentations on the SABR Fusion-Fission Hybrid Burner Reactor Concept

W. M. Stacey, Georgia Tech

An invited presentation "A Supplemental Fusion-Fission Hybrid Path to Fusion Power Development" was made to the Electric Power Research Institute's Fusion Energy Assessment Workshop in Palo Alto, CA on 7/21/11. This presentation may be found on this website under the "Policy" link on the homepage.

An invited tutorial lecture "Principles and Rationale of the Fission-Fusion Hybrid Burner Reactor" was presented at the FUNFI-11 Workshop on Fusion for Neutrons and Sub-Critical Nuclear Fission in Varenna, Italy on 9/13/11. This presentation may also be found on this website under the "Policy" link on the homepage.